Egyptian Informatics Journal 24 (2023) 161–172

Contents lists available at ScienceDirect

Egyptian Informatics Journal

journal homepage: www.sciencedirect.com

An analysis of 5G-MIMO communication system based SS for centralized cooperative and non-cooperative users

Waleed Algriree [a,*], Nasri Sulaiman [b,*], Maryam M. Isa [c], Ratna K.Z. Sahbudin [d], Siti L.M. Hassan [e], Emad Hmood Salman [f]

[a] Department of Computer and Communication Systems Engineering, Faculty of Engineering, Universiti Putra Malaysia, Serdang 43400, Selangor, Malaysia
[b] Department of Electrical and Electronic Engineering, Faculty of Engineering, Universiti Putra Malaysia, Serdang 43400, Selangor, Malaysia
[c] Department of Electrical and Electronic Engineering, Faculty of Engineering, Universiti Putra Malaysia, Serdang 43400, Selangor, Malaysia
[d] Department of Computer and Communication Systems Engineering, Faculty of Engineering, Universiti Putra Malaysia, Serdang 43400, Selangor, Malaysia
[e] Faculty of Electrical Engineering, Universiti Teknologi MARA, Selangor, Malaysia
[f] Department of Communications Engineering, College of Engineering, University of Diyala, Baquba, Diyala, Iraq

ARTICLE INFO

Article history:
Received 3 August 2022
Revised 23 December 2022
Accepted 22 February 2023
Available online 1 March 2023

Keywords:
5G-MIMO
Centralized cooperative network
F-OFDM-MIMO
FBMC-MIMO
Hann window
UFMC-MIMO

ABSTRACT

The purpose of 5G-MIMO communication systems is to boost the intensity of the received signal, and facilitate the application of the users' apparatus. However, in band-grabbing systems such as these, the accessibility of a spectrum is hindered by gridlocks. Also, to be considered is the spectrum's waveform, which is the type that contends with 5G networks specifically. This undertaking involves the development of a 5G-MIMO communication system based SS, in which the spectrum is enhanced, by way of a spectrum sensing (SS) algorithm. By replicating the energy detection procedure, this recommended SS algorithm engages the cosine law to filter the traffic signal, and subsequently portions it using the Welch algorithm. The Hann algorithm is then utilized, to window the traffic signal, to damp the high power delivered to the MIMO. The key role, of the SS algorithm, is to sense a spectrum for 5G-MIMO communication system, with the capacity to damp the MIMO effect for a variety of waveforms. The SS algorithm expressions are applicable for both non-cooperative and centralized cooperative users. For each expression, an examination was performed for waveforms used by 5G-MIMO communication systems. This included filtered-orthogonal frequency division multiplexing (F-OFDM), universal filtered multi-carrier (UFMC), and filter bank multi-carrier (FBMC) waveforms. The operating parameters, including SNR, the signal span and power, the antenna count, as well as the types of modulation for both non-cooperative and centralized cooperative users, were scrutinized. The simulation results revealed a notable achievement for the parameters lower than zero dB of SNR, greater than 95% global detection probability, less than 1% global system error probability, and less than 1% global false alarm probability. An evaluation of the recommended system's parameters discloses its superiority, in comparison to other previously developed systems.

1. Introduction

The recent unveiling of the 5G system, gives rise to the potential for a greater data size, a larger number of users, a shorter latency period, and an extended battery life [1]. However, the greater capacity of wireless networks, led to an increase in the introduction of up-to-date applications and services, which in turn led to a deficiency in spectrum. To exacerbate the situation, the spectrum's resources are limited, while its availability is rigidly programmed [2]. Among the effective routes for accessing the spectrum is by way of a Cognitive Radio Network (CRN). A CRN allows Secondary (unlicensed) Users (SUs), to reprocess the princi-

* Corresponding authors at: Department of Electrical and Electronic Engineering, Faculty of Engineering, Universiti Putra Malaysia, Serdang 43400, Selangor, Malaysia. (N.Sulaiman); Department of Computer and Communication Systems Engineering, Faculty of Engineering, Universiti Putra Malaysia, Serdang 43400, Selangor, Malaysia.(W.Algriree)

E-mail addresses: wkh_portsmouth@yahoo.com (W. Algriree), nasri_sulaiman@upm.edu.my (N. Sulaiman), maryam@upm.edu.my (M.M. Isa), ratna@upm.edu.my (R.K.Z. Sahbudin), sitilailatul.mohdhassan@yahoo.com (S.L.M. Hassan), emad_salman_eng@uodiyala.edu.iq (E.H. Salman).

https://doi.org/10.1016/j.eij.2023.02.003
1110-8665/

pal spectrum, left unexploited by its Primary (licensed) Users (PUs) [3].

Spectrum Sensing (SS), which is among the central roles of the CRN, involves the detection of a spectrum, followed by its examination, to determine if it is being used by a PU, or is inactive. Energy Detection (ED), cyclostationarity feature detection, waveform detection, and Matched Filter Detection (MFD), are among the detection algorithms applied for the detection process. In terms of structure and calculation intricacy, ED is considered the most straightforward, while MFD is looked upon as the most complicated. Though easy to apply, the ED algorithm is saddled with a poor performance, under the influence of noise deviations. Conversely, while the MFD algorithm is more intricate to apply, its level of efficiency is considerably higher [4]. The use several antennas, for the transmission and acceptance of a single signal, renders the Multiple-Input Multiple Output (MIMO) concept most efficient, for receiving the information-carrying PU signal. The application of the MIMO concept, equips the SS algorithm, with the capacity to overcome problems posed by the Signal-to-Noise Ratio (SNR), as well as issues related to the interface [5].

According to reports in relevant literature, several previous studies focused on merging the SS algorithms with the 5G-MIMO communication system to enhance the spectral exploitation, while reducing the likelihood of interference. This will serve to improve the detection process. A study conducted in 2019, focusing on the 5G-MIMO based Non-Orthogonal Multiple Access (NOMA) approach [6], employed the standard ED for both the NOMA and Orthogonal Multiple Access (OMA) concepts. According to the findings from this investigation, with regards to detection, the NOMA approach outperforms that of the OMA. However, the detection capacity was observed to be disappointing for SNR < −5 dB. In 2020, researchers came up with a MIMO process, based on a SS hybrid mixture model [7]. This process entailed the application of the Gaussian mixture model, on the whale and elephant herd optimization algorithms. The objective was to enhance the potential for detection, by reducing the likelihood of false alarms. However, as the least likelihood of a false alarm is above 0.47, the detection capacity was observed to be poor, particularly when it comes to a reduced SNR. The year 2020 also saw researchers examining a conventional probability ratio test [8]. This involved the use of ED and MFD algorithms, to apply the MIMO process on unidentified channel state information. While the findings from this effort point to a favourable performance for high SNR identification, the same cannot be said for SNR below 0 dB. In the same year, in keeping with the MIMO concept, authors in [9] recommended a SS algorithm, for the application of IoT. The detection process, of this algorithm, is based on its kernelizing of the Gaussian noise. In terms of detection capacity, the findings derived through simulation, disclosed an outstanding identification performance for 150 of the SNR > −6 dB samples. As for the other samples, the identification performance was observed to be unsatisfactory. In 2021 [10–11] and 2022 [12] researchers investigated several areas of the ED algorithm. These investigations involved the use of the 5G communication system, with the MIMO procedure. To sense orthogonal-frequency-division-multiplexing, the researchers in [10] scrutinized the conventional ED algorithm. The detection capability here, proved to be highly dependable, for an extensive antenna count (which is similar to the transmitter and receiver count), an extended span of the received PU signal, and SNR above −15 dB. However, this approach is not without its drawbacks. For instance, the expenditure rises in tandem with the increase in the antenna count, the PU signal span is constrained by conditions, and when it comes to SNR below −15 dB, the detection capacity is left wanting. In terms of the received PU signal, the researchers in [11] relied on a uniform span and power. According to their findings, the capacity of the ED algorithm for 5G-MIMO communication system for detection is noteworthy for 2 transmitter antennas and 4 receiver antennas, as well as SNR exceeding −15 dB, with the QPSK mapper type. Under other conditions, the detection capability was deemed poor. And lastly, the researchers in [12] delved into the ED algorithm threshold effect, with regards to the MIMO communication system. This investigation considered a variety of SNR levels, to scrutinize the threshold effect on performance capacity, derived by way of the ED algorithm. In the context of detection and the likely occurrence of false alarms, the capacity attributed to [12], was observed to be superior to that of [10] and [11]. Nevertheless, in the final analysis, [12] demonstrated a poor performance for SNR below −5.6 dB.

The studies described above, were aimed at enhancing the detection process, through the application of multi-branch diversity, for the transmitter and receiver. Several drawbacks, however, remain unresolved. These include a poor detection capability (elevated false alarm possibility) in a depleted SNR situation, the possibility of an extensive flaw in the system, and the high expenditure attributed to the considerable antenna count. Taking these drawbacks into consideration, we recommend an innovative cascading sensing system, which comprises a cosine filter, a Welch periodogram and Hann windowing. In this system's first stage, the intensity of the 5G-MIMO traffic signal is boosted, in the second stage the noise variance is reduced, and in the third stage the resolution of the MIMO traffic signal is enhanced. 5G-MIMO traffic signal is enhanced. With this undertaking we put forward:

- The numerical interpretation expressing of the recommended cascading sensing algorithm, in relation to several 5G waveform types, including F-OFDM-MIMO, UFMC-MIMO, and FBMC-MIMO signals.
- The extension of the recommended cascading sensing algorithm, for the detection of preceding 5G system waveform types, through for the crafting of a 5G-MIMO transmission system.
- An examination of the 5G-MIMO system, with regards to users, both non-cooperative and centralized cooperative.
- The graphical and numerical findings portraying the effects of noise variance, signal span, antenna count, different sorts of waveforms, and the mapper variety.

The rest of the paper is arranged as follows: Section 2 provides representations of the 5D signals considered for this paper, which are the F-OFDM, FBMC, and UFMC waveforms. The sensing of the F-OFDM-MIMO, FBMC-MIMO, and UFMC-MIMO signals, achieved through the development of the recommended SS mathematical model, based on the hybrid filter, is described in Section 3. In Section 4, the obtained results are introduced and discussed. Finally, in Section 5, the conclusion is presented.

2. Formulation the proposed 5G-MIMO systems based SS concept

A variety of signal contenders are available, for surmounting the restrictions, hampering previously developed 5G communication systems. These types of signals include the filtered-OFDM (F-OFDM), the universal filtered multi-carrier (UFMC), and the filter bank multi-carrier (FBMC) [13–15]. The transmitters of the F-OFDM-MIMO, the FBMC-MIMO, and the UFMC-MIMO systems, are scrutinized in this section. The representations that applied for this paper, are as defined in Table 1. The PU antenna count for all the systems is symbolized m (m = 1, 2, … M), and regarded a transmitter. As for the SU antenna count, this is symbolized r (r = 1, 2, … R), and regarded a receiver.

Table 1
The Description of Notations.

Notation	Description
H_0	Null hypothesis
H_1	Alternative hypothesis
$x(n)$	Transmitted 5G-MIMO (PU) signal (it is either F-OFDM, UFMC, or FBMC)
P_{fa}	Probability of false-alarm
P_d	Probability of detection
$y(n)$	Received 5G-MIMO (PU) signal
$\omega(n)$	Noise
$h(n)$	Channel gain
N	Original received signal length
σ_ω^2	Noise variance
σ_x^2	Received signal variance
λ	Decision statistic
η	Predefined threshold
$Q(.)$	Tail probability related to the standard normal distribution
$g_b[l]$	Frequency corresponding to the finite impulse response prototype filter
b^{th}	Block index with length l
C_P	Cyclic prefix size
$s_{d,v}^b$	Transmitted data for F-OFDM-MIMO signal
v^{th}	Subcarrier index
d^{th}	Sub-symbol index
$x_{F\text{-}OFDM\text{-}MIMO}[n]$	Transmitted F-OFDM-MIMO signal
$Y_{F\text{-}OFDM\text{-}MIMO}[k]$	Transformed of received F-OFDM-MIMO signal
$x_{UFMC\text{-}MIMO}[n]$	Transmitted UFMC-MIMO signal
$Y_{UFMC\text{-}MIMO}[k]$	Transformed of received UFMC-MIMO signal
$x_{FBMC\text{-}MIMO}[n]$	Transmitted FBMC-MIMO signal
$Y_{FBMC\text{-}MIMO}[k]$	Transformed of received FBMC-MIMO signal
$Y'_{F\text{-}OFDM\text{-}MIMO}[k]$	Transformed of received F-OFDM-MIMO signal without null coefficients
$Y'_{UFMC\text{-}MIMO}[k]$	Transformed of received UFMC-MIMO signal without null coefficients
$Y'_{FBMC\text{-}MIMO}[k]$	Transformed of received FBMC-MIMO signal without null coefficients
s_v^b	Transmitted data for UFMC-MIMO signal
$g[l]$	Frequency corresponding to the finite impulse response prototype filter
$\varphi_{d,v}$	Additional phase term that was described as $(d + v)\ \pi/2$.
$s_{d,v}$	Transmitted data for FBMC-MIMO signal
q	Sub-carriers for FBMC-MIMO system
P	Transmitter power
M	Number of transmitted antennas
R	Number of received antennas
$\mathbb{Z}$	Magnitude of complex vector
$Var[\cdot]$	The variance operator
$E[\cdot]$	The expectation operator
K	Transformed received signal length (corresponding to the original received signal length)
K'	New transformed received signal length after removing null coefficients
ξ	Ratio of original signal length to the new signal length
$nseg$	Number of Welch segments
$lseg$	Length of every segment
PSD	Power spectral density of every segment
$RPSD$	Resultant of power spectral density of every segment
$Han[.]$	Hann window function
Q_{fa}	Probability of false-alarm for cooperative users
Q_d	Probability of detection for cooperative users
NS	Number of secondary users
α	SNR
ROC	Receiver operating characteristic

For the F-OFDM-MIMO system, it is described in the Fig. 1 and is formulates as,

$$x_{F-OFDM-MIMO}[n] = \sum_{m=0}^{M-1}\sum_{b=0}^{B-1}\sum_{d=0}^{D-1}\sum_{l=0}^{L-1}\sum_{v=0}^{V-1} s_{d,v}^b g_b[l] e^{j2\pi n\frac{(v-l-dC_P)}{V}} \quad (1)$$

where $g_b[l]$ represents the frequency that corresponds to the finite impulse response prototype filter for b^{th} block with length l, and the cyclic prefix size is denoted by C_P, $s_{d,v}^b$ denotes TX data for the b^{th} block, v^{th} subcarrier, and d^{th} sub-symbol.

On the other hand, The UFMC-MIMO system may be formulated as Equation (2) as follows:

$$x_{UFMC-MIMO}[n] = \sum_{m=0}^{M-1}\sum_{b=0}^{B-1}\sum_{l=0}^{L-1}\sum_{v=0}^{V-1} s_v^b g[l] e^{j2\pi n\frac{(v-l)}{V}} \quad (2)$$

where s_v^b denotes the TX data, and $g[l]$ represents the frequency value that corresponds to the finite impulse response filters. Fig. 2 describes the UFMC-MIMO system.

The last but not least, the FBMC-MIMO system is described in Fig. 3, and Equation (3) defines this system as,

$$x_{FBMC-MIMO}[n] = \sum_{m=0}^{M-1}\sum_{d=-\infty}^{\infty}\sum_{v=0}^{V-1} s_{d,v} g[q - d\frac{V}{2}] e^{j2\pi n\frac{q}{V}} e^{j\varphi_{d,v}} \quad (3)$$

wherein: $\varphi_{d,v}$ denotes the additional phase term that is described as $(d + v)\pi/2$, the $s_{d,v}$ is valued if the two components of the symbol (real and imaginary) is transmitted with the delay and q sub-carriers.

Suppose that P_m denotes the transmitter power, which is allocated to the m-th antenna factor. Each separate signal $\boldsymbol{x}_m$, transmitted by way of the m-th transmitter antenna, is deemed an intricate signal, represented as $\boldsymbol{x}_m = x_m + jx_m$ [16]. Accordingly, every signal transmitted by way of the M transmitter antennas, by a distinct PU, is represented as:

$$P = \sum_{m=1}^{M} P_m \quad (4)$$

$$x = \sum_{m=1}^{M} \boldsymbol{x}_m \quad (5)$$

Alternatively, the receiver (SU) taking delivery of the Equation (5) signal, by way of the r-th antenna, with n samples (n = 1, 2, ... N) is represented as:

$$y(n) = \begin{cases} \omega(n) \\ h(n)x(n) + \omega(n) \end{cases} \quad (6)$$

in which $x(n)$ denotes the complex magnitude $\mathbb{Z}$ vector, of the transmitter 5G signal. The intricate noise sample at the r-th receiver antenna, denoted $\omega(n)$, is regarded an additive white Gaussian noise (AWGN), which comes with a zero mean and noise variance, $\sigma_\omega{}^2$, for circular symmetric distribution $\mathcal{N}$ $(0, 2\sigma_\omega{}^2(n))$. $h(n)$ is a complex vector of magnitude $\mathbb{Z}^{1\times M}$, which signifies the channel gain, between the M transmitter antennas, and the r-th receiver antenna [17]. As such, the SNR value (α), at the r-th antenna of SU, at every R receiver antenna, and the average SNR value, is represented as in Equations (7), (8) and (9) correspondingly [18]:

$$\alpha(n) = \frac{|h(n)|^2 \frac{1}{N}\sum_{n=1}^{N}|x(n)|^2}{2\sigma_\omega^2(n)} \quad (7)$$

$$\alpha = \sum_{r=1}^{R} \alpha_r(n) \quad (8)$$

$$\bar{\alpha} = \alpha/R \quad (9)$$

Consequently, the expression of Equation (4), with regards to SS is:

$$Y(n) = \begin{cases} \sum_{r=1}^{R}\omega(n) : H_0 \\ \sum_{r=1}^{R}h(n)x(n) + \sum_{r=1}^{R}\omega(n) : H_1 \end{cases} \quad (10)$$

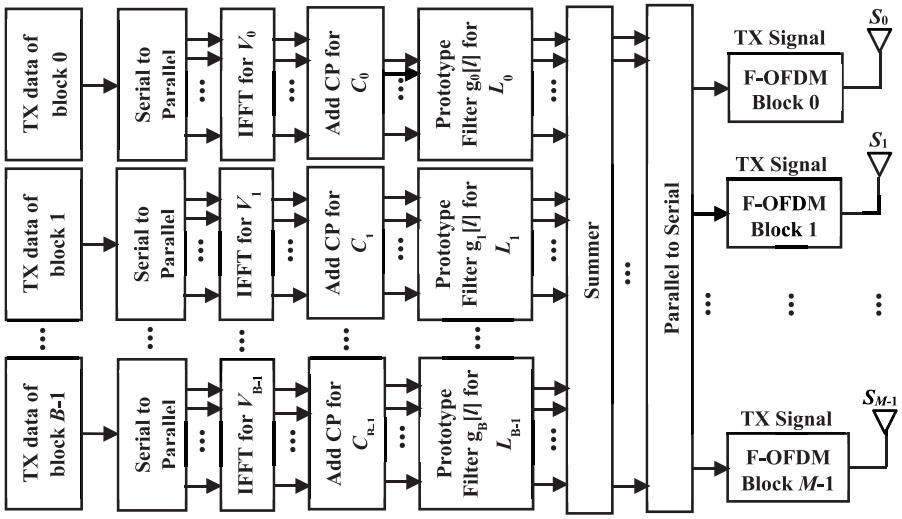

Fig. 1. F-OFDM-MIMO system block diagram with *M* TX branches.

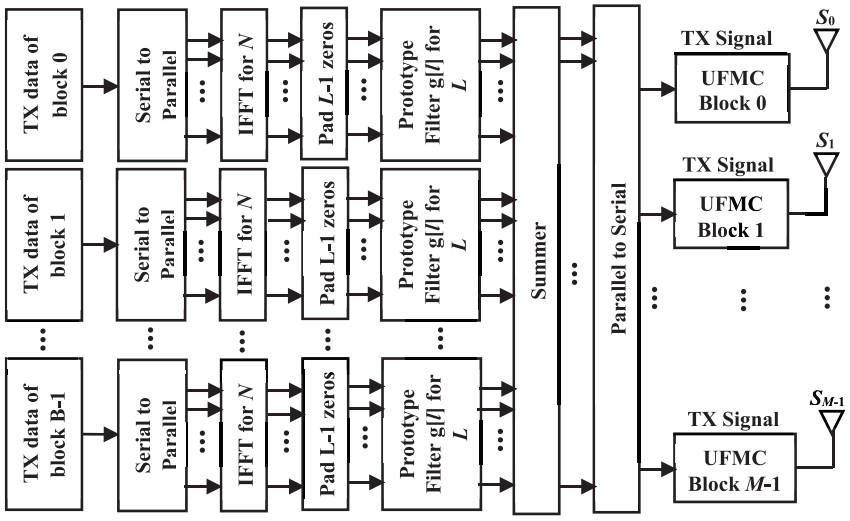

Fig. 2. UFMC-MIMO system block diagram with *M* TX branches.

in which the hypotheses H_0 and H_1 signify the absence (non-existence) and presence (attendance) of the PU signal correspondingly. The SS procedure involves the corroboration of one of these hypotheses. Put simply, the presence of the PU indicates the validity of the hypothesis H_1, while the absence of PU indicates the validity of hypothesis H_0. Additionally, $Y(n)$ signifies the general signal delivered to the SU R receiver antennas, during the n-th spectrum episode. The selection of the hypothesis is determined by the signal's received intensity, at the SU site. The PU signal is considered present, and hypothesis H_1 with regards to Equation (10) is verified, when the received signal's energy is above the threshold. In a situation where the received signal is below the predetermined threshold, the PU signal is deemed absent, allowing the SU to exploit the spectrum, as hypothesis H_0 will be considered authenticated. In the context of signal transmission, the outcomes of the hypothesis authentication process, serve to ascertain the impending exploits of the SU.

Following the acquirement of the received signal, or predefined-threshold (η) for R, with regards to the F-OFDM-MIMO, the FBMC-MIMO, and the UFMC-MIMO systems, the receiver antennas are squared as demonstrated below:

$$\eta = \sum_{r=1}^{R} \sum_{n=1}^{N} |y(n)|^2 \tag{11}$$

The ultimate pronouncement, with regards to the absence or presence of the PU signal, is arrived at through an evaluation of the hypotheses H_0 and H_1, by way of comparison with the test statistic (λ) as the following equation:

$$\eta(n) < \lambda(n) : H_0$$

$$\eta(n) > \lambda(n) : H_1 \tag{12}$$

Due to the overwhelming number of samples that come with the F-OFDM-MIMO, FBMC-MIMO, and UFMC-MIMO systems, the test statistic attributed to Equation (11), can be estimated as a typical distribution, in the following manner:

$$\lambda(n) \; \mathcal{N}\left(\begin{array}{c} \sum_{r=1}^{R} \sum_{n=1}^{N} E\left[|y(n)|^2\right], \\ \sum_{r=1}^{R} \sum_{n=1}^{N} Var\left[|y(n)|^2\right] \end{array} \right) \tag{13}$$

in which the variance operator is represented as $Var[\cdot]$, and the expectation operator is represented as $E[\cdot]$. The non-static nature of the wireless channel, does not exempt it from the effects of various issues, including noise, fading, shadowing, and interference over time. To reduce the level of difficulty, and facilitate the execution of mathematical modelling, the channels are deemed stationary, throughout the N samples detection procedure [17,18].

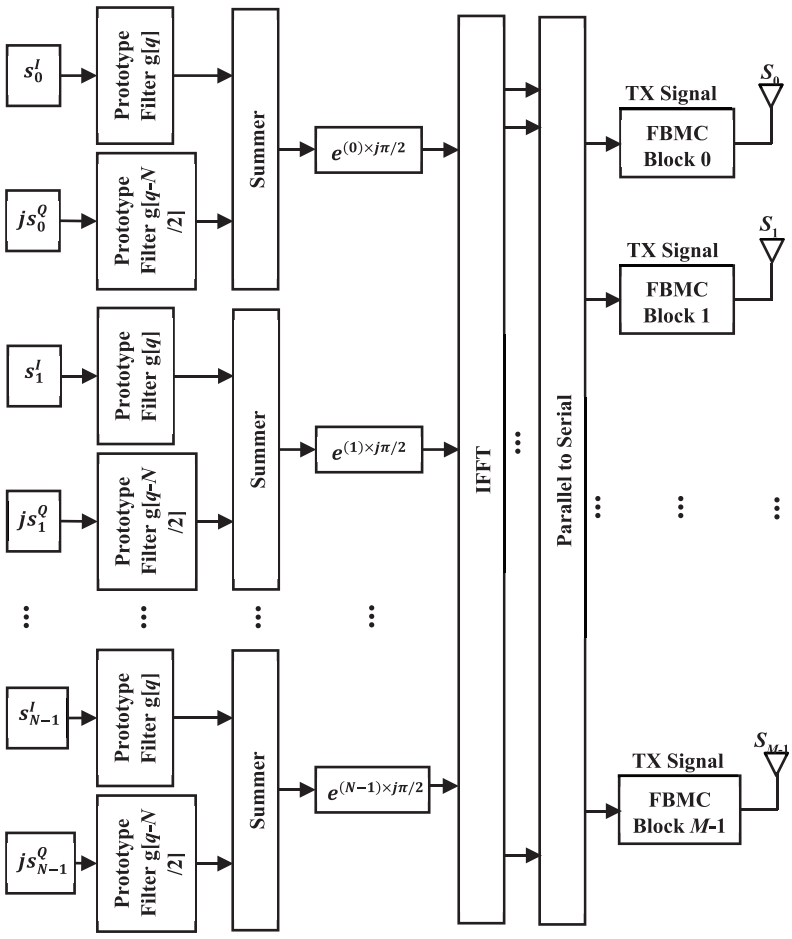

Fig. 3. FBMC-MIMO system block diagram with *M* TX branches.

Thus, if during each spectrum sensing episode n, the signal's channel gain $h(n)$, delivered to the r-th receiver antenna, can be taken to be unvarying, the channel gain can be put across as $h(n) = h$, with h standing for the intricate channel gain matrix, for all antennas of the R receiver. Also, by considering the noise variance received at the r-th receiver to be unvarying [17,18], the noise variance can be expressed as $2\sigma^2{}_{\omega}(n) = 2\sigma^2{}_{\omega}$.

As for the energy detection procedure, there is no necessity for any previous information regarding the PU signal. The entire immediate power, of the PU during the n-th sensing episode, is in proportion to all signals (with the variance $2\sigma^2{}_{xr}(n)$), delivered to the R receiver antennas [17,18]. This is expressed as:

$$P = \sum_{r=1}^{R} |h|^2 2\sigma^2_{xr}(n) \tag{14}$$

where

$$2\sigma^2_{xr}(n) = \frac{1}{N}\sum_{n=1}^{N} |x_r(n)|^2 \tag{15}$$

3. Formulation the 5G-MIMO systems based proposed SS technique

3.1. The impact of detection parameters for 5G-MIMO systems

The parameters for the probability of detection (P_d), and the probability of false alarm (P_f), are frequently applied, for assessing the SS performance, in terms of non-cooperative users as described in Equations (16) and (17). The P_f, is described as the likelihood of the SU, wrongly proclaiming the transmission of a licensed user (PU), when in fact, the spectrum is devoid of a PU [19,20].

$$P_{fa} = Q\left(\frac{\eta - \sigma_w^2}{\sqrt{\frac{2}{N}}\sigma_w^2}\right) \tag{16}$$

$$P_d = Q\left(\frac{\eta - (\sigma_x^2 + \sigma_w^2)}{\sqrt{\frac{2}{N}}(\sigma_x^2+\sigma_w^2)}\right) \tag{17}$$

in which Q denotes the Tail probability, associated to the conventional typical distribution. The application of the SS technique, for the recommended F-OFDM-MIMO, FBMC-MIMO, and UFMC-MIMO systems, for the false alarm probability, in accordance with energy detection, Equation (16) is expressed as:

$$P_{fa} = Q\left(\frac{\lambda - R(2\sigma_\omega^2)}{\sqrt{\frac{8R}{N}(\sigma_\omega^2)^2}}\right) \tag{18}$$

An elevation, in the false alarm probability, is an indication that the window for spectrum utilization, by the SU, during intervals when the PU is inactive, has been bypassed. It is essential, that the false alarm probability be reduced to the minimum, so that the efficiency of the spectrum can be raised, to the highest level possible [20]. As can be gathered from Equation (18), the threshold,

the receiver antenna count, the sample count in the detection procedure, and the noise variance, influences the probability of a false alarm.

Detection probability, on the other hand, refers to the likelihood that the SU rightly proclaims the presence of a licensed user, when the PU is truly present, and exploiting the spectrum for transmission [20]. As for the recommended F-OFDM-MIMO, FBMC-MIMO, and UFMC-MIMO communication systems, the performance of SS through energy detection, by way of the squaring technique, Equation (17) is expressed as:

$$P_d = Q\left(\frac{\lambda - 2R(\sigma_x^2 + \sigma_\omega^2)}{\sqrt{\frac{8R}{N}(\sigma_x^2 + \sigma_\omega^2)^2}}\right) \tag{19}$$

A raised detection probability is beneficial, as it improves spectrum usage, and the SU's detection capacity. According to Equation (19), other than the probability of a false alarm, the realization of a greater detection probability, also hinges on several parameters. These include the total sample count involved in the detection process, the PU's transmitter power, the antenna count engaged by the SU for SS, and the noise variation at the position of the SU.

As demonstrated by the link between Equations (18) and (19), the feasible execution of detection, requires a verification regarding the absence or presence of a PU signal. Establishing the route, to identifying the best threshold selection procedure, remains among the major goals, in the SS domain. The recommendations for a threshold selection procedure range from the detection process, in accordance with the rapid and immediate changes of the noise variation levels, to the establishment of a set threshold, in accordance with predetermined parameters, such as the constant false alarm probability. For instance, the IEEE 802.22 focuses on predetermined false alarm probability to arrive at $Pf < 0.1$ [19]. In accordance with the specified false alarm probability concept [21], the receiver antenna count, and the noise variance, the threshold definition by Equation (18) is expressed as:

$$\lambda = R(2\sigma_\omega^2) + \sqrt{\frac{8R}{N}(\sigma_\omega^2)}Q^{-1}(P_{fa}) \tag{20}$$

Furthermore, as the $Q^{-1}(.)$ function comes with a monotonically declining activity, the rise in the sample count during SS, ensures the detection of signals with exceedingly depleted SNRs, in situations where there is perfect knowledge with regards to noise power. The sample count (N), considered during the specified false alarm probability concept [21], to distinguish the PU signal, is a significant parameter, for meeting the conditions, of the anticipated false alarm probability. By referring to relation (18), the least number of samples (N) can be distinguished for the specified detection probability, the false alarm probability, the SNR, and the R receiver antenna count. The expression for the minimum number of samples, which is not a function of the detection threshold, is as follows:

$$N = 8R(\sigma_\omega^2)\left(\frac{Q^{-1}(P_{fa})}{\lambda - R(2\sigma_\omega^2)}\right)^2 \tag{21}$$

A rise in the number of samples, however, also leads to an extension in the sensing period, which represents the main shortcoming of the squaring technique. This is because at depleted SNRs, a substantial sample number count is essential, for an accurate detection. An extension in the sensing duration, however, can lead to implementation issues, as certain systems come with a predetermined sensing period (the maximum sensing duration for IEEE802.22 systems, for instance, is 2 s). Any increase in the sensing period will take its toll on the battery life of power-dependent mechanisms (such as sensors) operating in an IoT setting. Determining the appropriate number of samples, for an accurate detection, is among the challenges associated to the optimization process [22].

3.2. The impact of proposed SS technique for 5G-MIMO systems

Transmission issues associated to spectral effectiveness, flexibility, inactivity, intricacy, and power usage, can be managed through the 5G system. Regular facilities can be rendered more organized, as the system advocates frequency bands, and promotes network diversity. The waveform of 5G is also held in high regard, when it comes to improvements related to interface flexibility, among network usage participants. On other hand, the 5G communication system can exploit the benefits of MIMO technique with three waveform technologies [23]. This section describes 5G-MIMO systems based SS to facilitates the availability of spectrum services for three different waveforms, with the SU sensing each waveform for non-cooperative users (Fig. 4), and centralized coop-

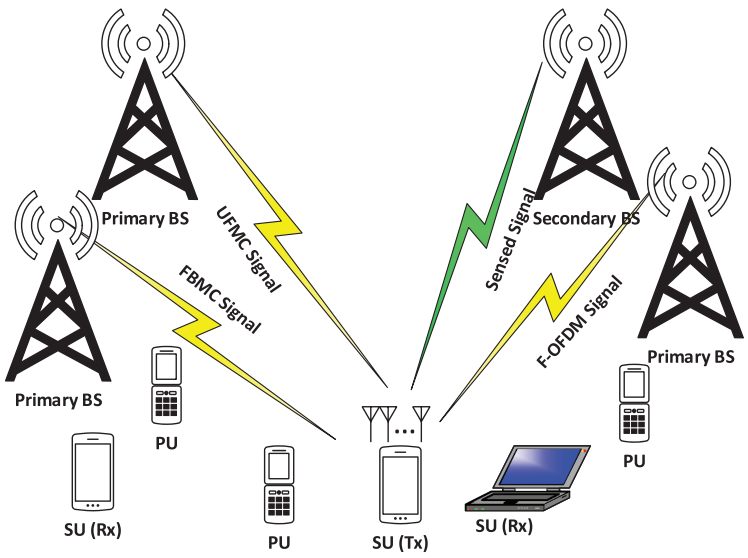

Fig. 4. 5G-MIMO system with M TX branches and various waveforms for non-cooperative users.

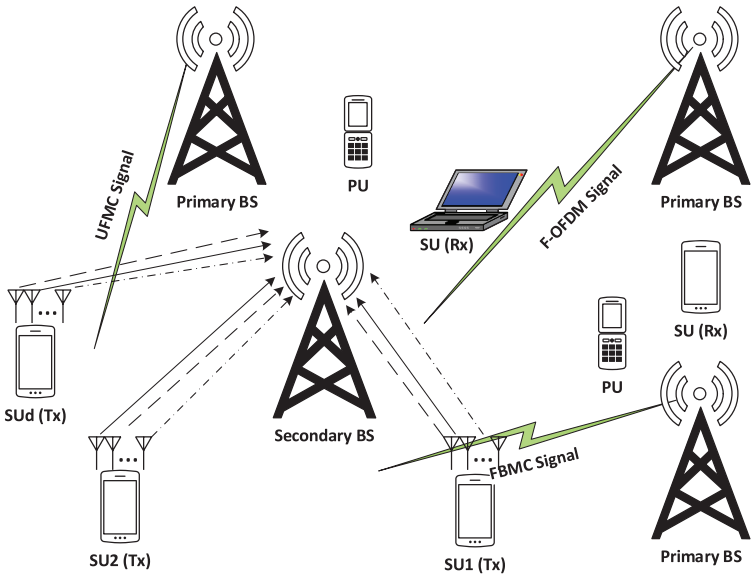

Fig. 5. 5G-MIMO system with *M* TX branches and various waveforms for centralized cooperative users.

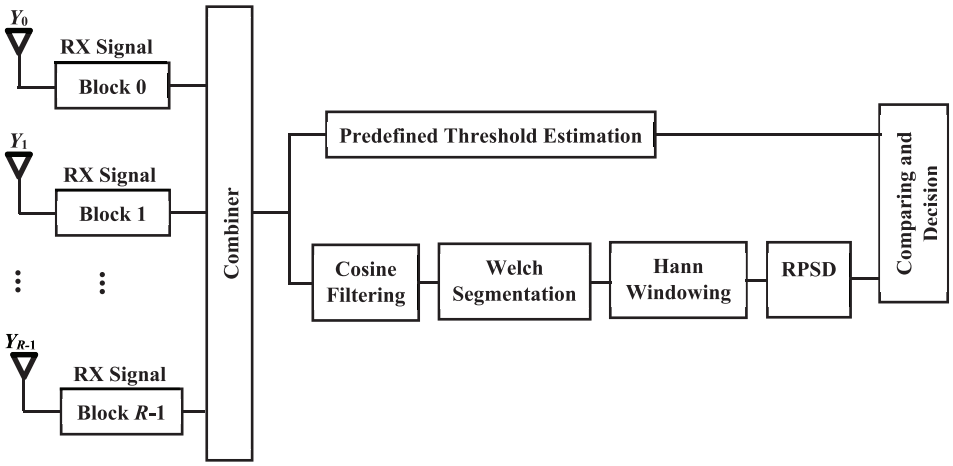

Fig. 6. The block diagram of the proposed detection technique for 5G-MIMO system.

erative users (Fig. 5). As the waveforms come with a variety of features, the recommended SS approach needs to be equipped with the capability, to accurately sense each waveform.

The recommended SS technique, for the previously cited 5G-MIMO waveform contenders, is portrayed in the block diagram of Fig. 6.

The restructured cosine filter is examined, for the crafting of the SS frequency domain scheme-based detection. This is expressed in following equations. The initial step involves the filtering of the received signal, using the cosine filter [24]:

$$Y[0] = \frac{\sqrt{2}}{N}\sum_{n=0}^{N-1} y[n], k = 0 \tag{22}$$

$$Y[k] = \frac{2}{N}\sum_{n=0}^{N-1} y[n]\cos\left(\frac{\pi k(2n+1)}{2N}\right), 1 \le k \le K-1 \tag{23}$$

Thus, the received 5G-MIMO (PU) signal, $y[n]$, becomes:

$$y[n] = \begin{cases} \omega[n] & H_0 \\ \begin{cases} x_{F-OFDM-MIMO}[n] \\ x_{UFMC-MIMO}[n] \\ x_{FBMC-MIMO}[n] \end{cases} + \omega[n] & H_1 \end{cases} n = 1, 2, \ldots, N \tag{24}$$

It is notable, that the 5G-MIMO received signals, which are either $x_{F\text{-}OFDM\text{-}MIMO}$, $x_{UFMC\text{-}MIMO}$, or $x_{FBMC\text{-}MIMO}$, are deemed autonomous, and in accordance with the indistinguishably disseminated (i.i.d) random procedure. $Y[k]$ denotes the corresponding filtered signal for $y[n]$. The second step entails the eradication of the $Y[k]$ null coefficients, to lessen both the mathematical intricacy, and the sensing spell. Consequently, $Y[k]$ is windowed with a fresh length of K', where $K' < K$ (i.e., the alteration of $Y[k]$ to $Y'[k]$) and traffic, is conveyed with the support of several samples. Both these steps are presented in Fig. 7.

According to Equation (24), Equation (25) depicts the altered F-OFDM signal by way of the cosine filter, which is followed by the elimination of all its null coefficients, as portrayed in Equation (26).

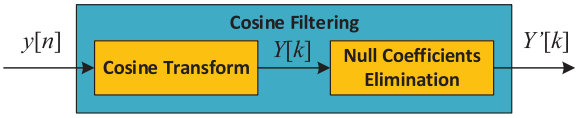

Fig. 7. Cosine transforming and null coefficients eliminating processes.

$$Y_{F-OFDM-MIMO}[k] = (-1)^k \sum_{m=0}^{M-1}\sum_{n=0}^{N-1}\sum_{b=0}^{B-1}\sum_{d=0}^{D-1}\sum_{l=0}^{L-1}\sum_{v=0}^{V-1} \times \frac{s_{d,v}^b g_b[l] e^{j2\pi n\frac{(v-l-dC_P)}{V}}}{\sqrt{N}} + \sqrt{\frac{2}{N}}\sum_{m=0}^{M-1}\sum_{n=0}^{N-1}\sum_{b=0}^{B-1}\sum_{d=0}^{D-1}\sum_{l=0}^{L-1}\sum_{v=0}^{V-1} s_{d,v}^b g_b[l] e^{j2\pi n\frac{(v-l-dC_P)}{V}} \times \cos\left(\frac{\pi k(2n+1)}{2N}\right), 0 \le k \le K-1 \quad (25)$$

$$Y'_{F-OFDM-MIMO}[k] = Y_{F-OFDM-MIMO}[k], 0 \le k \le K'-1 \quad (26)$$

Likewise, Equations (27) and (28) display the altered UFMC signal, and the eradication of its null coefficients, correspondingly.

$$Y_{UFMC-MIMO}[k] = (-1)^k \sum_{m=0}^{M-1}\sum_{n=0}^{N-1}\sum_{b=0}^{B-1}\sum_{l=0}^{L-1}\sum_{v=0}^{V-1} s_v^b g[l] e^{j2\pi n\frac{(v-l)}{V}}/\sqrt{N} + \sqrt{\frac{2}{N}}\sum_{m=0}^{M-1}\sum_{n=0}^{N-1}\sum_{b=0}^{B-1}\sum_{l=0}^{L-1}\sum_{v=0}^{V-1} s_v^b g[l] e^{j2\pi n\frac{(v-l)}{V}} \times \cos\left(\frac{\pi k(2n+1)}{2N}\right), 0 \le k \le K-1 \quad (27)$$

$$Y'_{UFMC-MIMO}[k] = Y_{UFMC-MIMO}[k], \ 0 \le k \le K'-1 \quad (28)$$

Equation (29) draws attention to the transformed FBMC signal, and Equation (30) demonstrates the deletion of its null coefficients.

$$Y_{FBMC-MIMO}[k] = (-1)^k \sum_{m=0}^{M-1}\sum_{n=0}^{N-1}\sum_{d=-\infty}^{\infty} \times \sum_{v=0}^{V-1} s_{d,v} g\left[q - d\frac{V}{2}\right] e^{j2\pi n\frac{v}{V}} e^{j\varphi_{d,v}}/\sqrt{N} + \sqrt{\frac{2}{N}} \times \sum_{m=0}^{M-1}\sum_{n=0}^{N-1}\sum_{d=-\infty}^{\infty}\sum_{v=0}^{V-1} s_{d,v} g[q - d\frac{V}{2}] e^{j2\pi n\frac{v}{V}} e^{j\varphi_{d,v}} \times \cos\left(\frac{\pi k(2n+1)}{2N}\right), \ 0 \le k \le K-1 \quad (29)$$

$$Y'_{FBMC-MIMO}[k] = Y_{FBMC-MIMO}[k], \ 0 \le k \le K'-1 \quad (30)$$

Consequently, the *Pd* is acquired for the non-cooperative user, by way of the fresh length *K'*, in the following manner:

$$P_d = Q\left(\frac{\lambda - 2R(\xi\sigma_s^2 + \sigma_\omega^2)}{\sqrt{\frac{8R}{K'}(\xi\sigma_s^2 + \sigma_\omega^2)^2}}\right) \quad (31)$$

in which ξ depicts the previous signal length to fresh signal length ratio. This is expressed as,

$$\xi = \frac{N}{K'} \quad (32)$$

After the implementation of the cosine filter, *Y'*[*k*] was separated into *nseg* segments, with a *lseg* length, derived by way of the Welsh segmentation algorithm. This was followed by the computation of the PSD, for each segment, after they were individually windowed, with the utilization of the Hann window. Eventually, the consequential PSD (*RPSD*) was assumed the average of the previous PSDs. In the context of the decision statistic, this renders *RPSD* the regulating agent. This is portrayed in Fig. 8, where the expression 'seg' indicates segment, and 'winseg' indicates windowed segment.

The Hann window function, *Han*[.], is expressed as [24,25],

$$Han[\psi] = 0.5 - 0.5\cos\left(\frac{2\pi\psi}{\Psi - 1}\right), \quad 0 \le \psi \le \Psi - 1 \quad (33)$$

Its application, for each segment, is followed by the multiplication of every segment with the Hann window, to acquire *PSD*. This is expressed as follows

$$PSD^{(j)}[k] = \frac{1}{lseg}\left|\sum_{i=0}^{lseg} Y\prime[i] Han[i]\right|^2, \ 0 \le k \le K'-1, \ j = 1, 2, \cdots, nseg \quad (34)$$

in which *Y'* denotes *Y'F-OFDM-MIMO*, *Y'UFMC-MIMO*, or *Y'FBMC-MIMO*. The resulting PSDs are assessed through the following equation:

$$RPSD = \frac{1}{nseg}\sum_{i=0}^{nseg-1} PSD(i) = \lambda \quad (35)$$

Thus, the binary hypothesis determines H_0, whether λ is not more than, or equivalent to η, which is an indication that the received 5G-MIMO (PU) signal comprises solely noise. The binary hypothesis also determines H_1, whether λ is above η, which is an indication that the received 5G-MIMO (PU) signal comprises one of its candidates, as well as noise. This is expressed as:

$$\begin{cases} H_0, & \lambda \leqslant \eta \\ H_1, & \lambda > \eta \end{cases} \quad (36)$$

Next, to generalize the aforementioned proposed SS for *NS* SUs, the decision fusion application, by way of the OR scheme, for centralized-cooperative users, is expressed as:

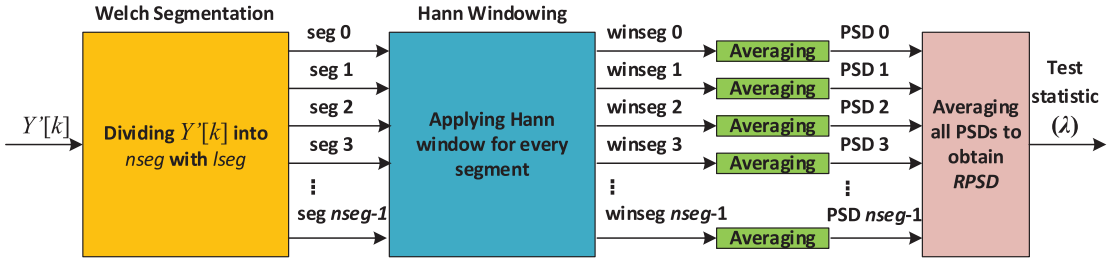

Fig. 8. The processes of segmenting and windowing.

$$Q_{fa} = 1 - \prod_{ns=1}^{NS} (1 - P_{fa}) = 1 - \prod_{ns=1}^{NS} \left(1 - Q \left(\frac{\lambda - R(2\sigma_{\omega}^2)}{\sqrt{\frac{8R}{N} (\sigma_{\omega}^2)^2}} \right) \right) \quad (37)$$

$$Q_{d} = 1 - \prod_{ns=1}^{NS} \left(1 - Q \left(\frac{\lambda - 2R(\xi\sigma_{s}^2 + \sigma_{\omega}^2)}{\sqrt{\frac{8R}{K'} (\xi\sigma_{s}^2 + \sigma_{\omega}^2)^2}} \right) \right) \quad (38)$$

in which Q_{fa} and Q_d signify the false alarm and detection probability values respectively, in relation to *NS*-th centralized-cooperative users.

4. Simulation results

In this section, the obtained results of the proposed systems have been presented by using the MathWorks® to execute the simulation of the F-OFDM-MIMO, UFMC-MIMO and FBMC-MIMO systems. For obtaining the detection performance of the abovementioned systems, the results are found with different SNR values and AWGN channels for various factors of the generated shapes of F-OFDM-MIMO, UFMC-MIMO and FBMC-MIMO systems. The properties of F-OFDM, UFMC, and FBMC signals of 5G, and the number of transmitter and receiver antennas are described in the Table 2. With the help of 10,000 trials of Monte Carlo simulation, the detection performance is obtained to validate the proposed SS technique. Thus, the data of different signals have been got by running this simulation.

4.1. The impact of proposed SS technique for non-cooperative users

This sub-section presents the detection performance of the proposed SS technique for the F-OFDM-MIMO, UFMC-MIMO and FBMC-MIMO systems. For only one SU, the detection performance is performed according to Equations (18) and (31). For Figs. 9, 10, and 11, the x-axis represents the probability of false alarm whereas the y-axis represents the probability of detection. Fig. 9 reveals the performance for the F-OFDM-MIMO system for different low SNR values and constant false alarm probability. Although the curves are obtained for various SNR values, they are conflict each other. The reason is the power of the MIMO antennas that improves the detection performance of the detection for this system. However, the long signal length in the UFMC-MIMO system does not help the proposed system for the −20 dB to be the perfect rate as shown in Fig. 10. Therefore, the number of antenna should be increased to enhance the detection performance to sense the signal with SNR < -20 dB. Fig. 11 describes the detection performance for the FBMC-MIMO system. The detection performance has been improved for 0 and −10 dB values of SNR more than that for −20 dB value of SNR. However, all performances are significant. The significant detection performance is defined by high detection probability with low false alarm probability. For SNR = 0 dB and short signal length, detection performance for the UFMC-MIMO system is bet-

Table 2
The properties of 5G-MIMO waveform types.

F-OFDM	FBMC	UFMC
Number of TX antenna = 2	Number of TX antenna = 2	Number of TX antenna = 2
Number of RX antenna = 2	Number of RX antenna = 2	Number of RX antenna = 2
Number of FFT = 1024	Number of FFT = 512	Number of FFT = 1024
Number of Resource Block = 50	Size of Sub-band = 20	Number of Guard = 212
Number of sub-carriers = 12	Number of sub-bands = 10	Overlapping Symbols = 4
Length of cyclic prefix = 72	Length of cyclic prefix = 43	Number of Symbols = 100
Bits / Sub-carrier = 6	Bits / Sub-carrier = 4	Bits / Sub-carrier = 2
Tone offset = 2.5	Sub-band offset = 156	
Length of filter = 513	Length of filter = 43	
64 QAM	16 QAM	4 QAM

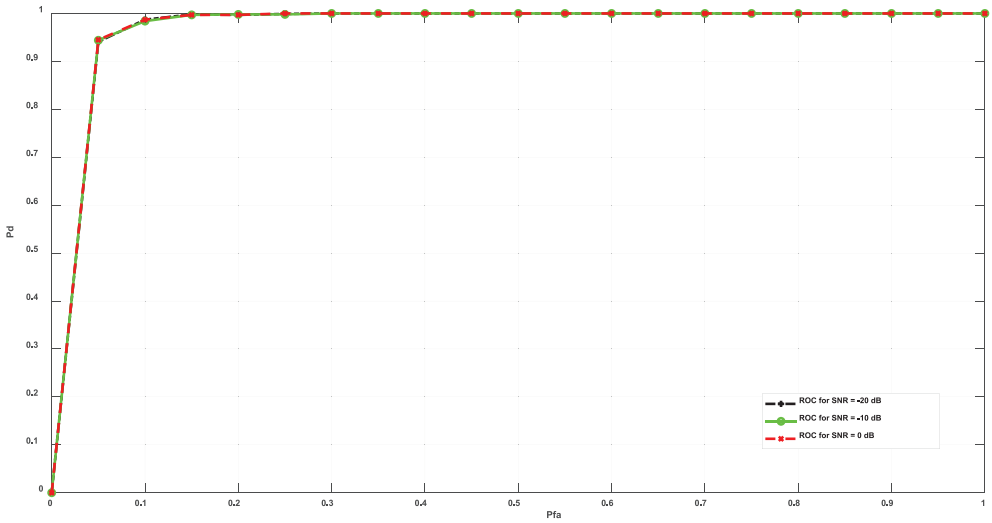

Fig. 9. The detection performance of proposed SS for F-OFDM-MIMO with non-cooperative users.

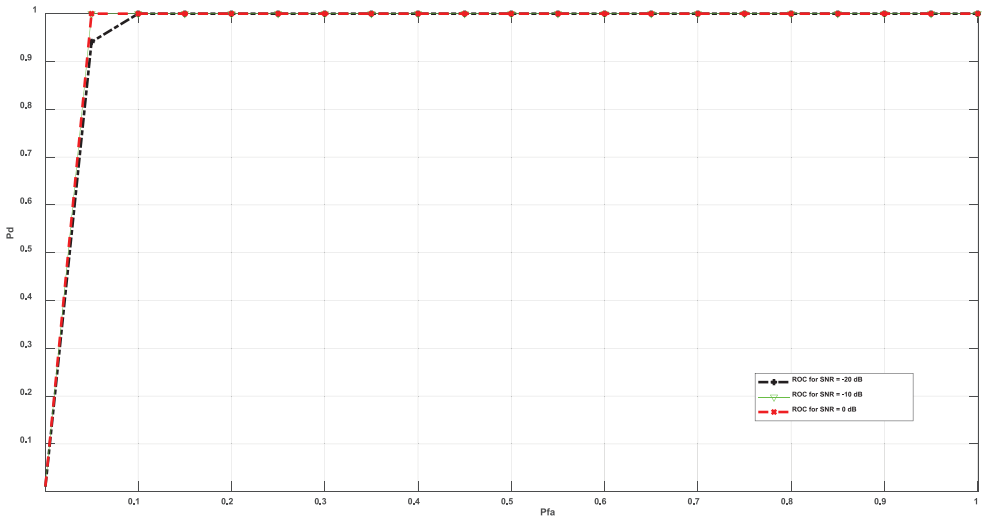

Fig. 10. The detection performance of proposed SS for UFMC-MIMO with non-cooperative users.

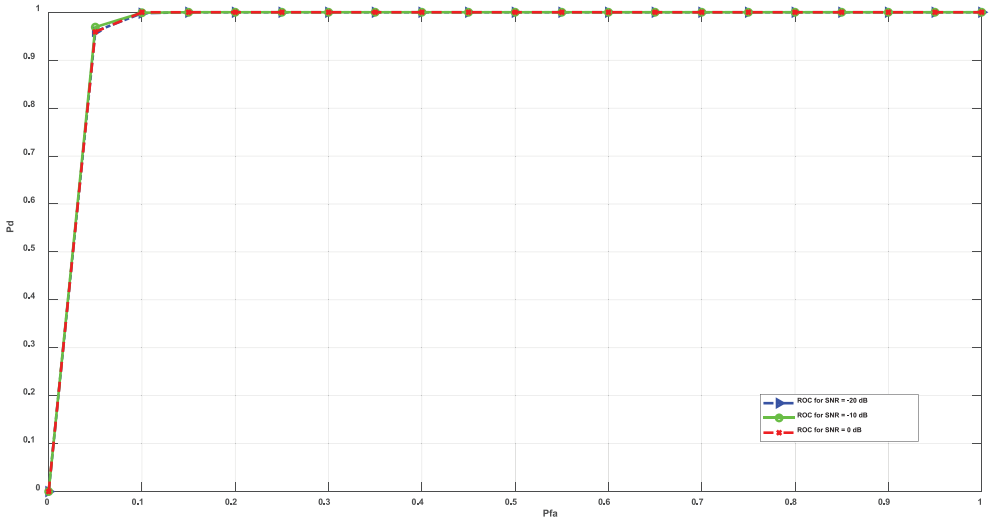

Fig. 11. The detection performance of proposed SS for FBMC-MIMO with non-cooperative users.

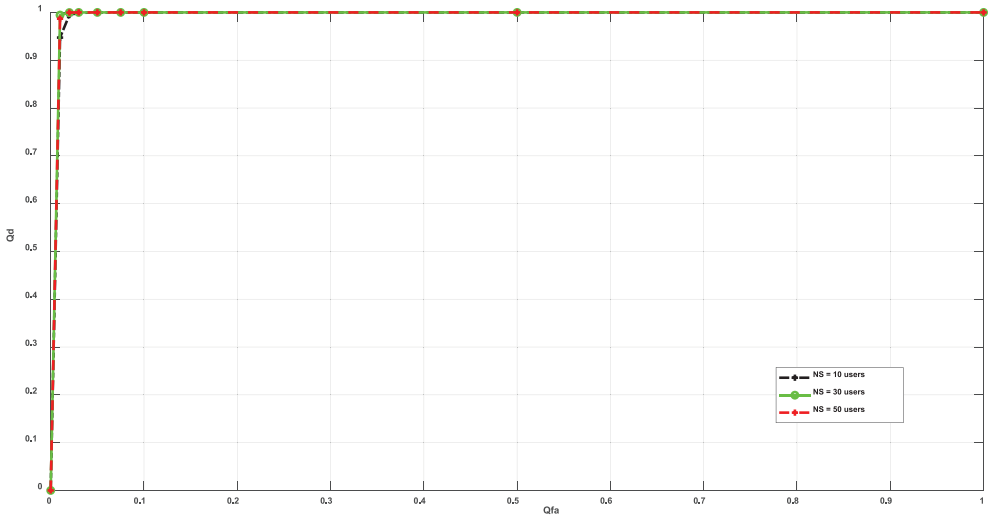

Fig. 12. The detection performance of proposed SS for F-OFDM-MIMO with centralized cooperative users.

ter than that other systems. However, the detection performance is also good for lower SNR.

4.2. The impact of proposed SS technique for centralized cooperative users

This sub-section presents the detection performance of the proposed SS technique for the F-OFDM-MIMO, UFMC-MIMO and FBMC-MIMO systems with many SUs. The numbers of SU, that are used in the simulation, are 10, 30, and 50 dB. The detection performance is obtained according to Equations (37) and (38). For Figs. 12, 13, and 14, the x-axis represents the probability of global false alarm whereas the y-axis represents the probability of global detection. The performance is obtained for constant value of SNR, number of SUs, and global false alarm probability. Fig. 12 reveals the detection performance of F-OFDM-MIMO system for −20 dB

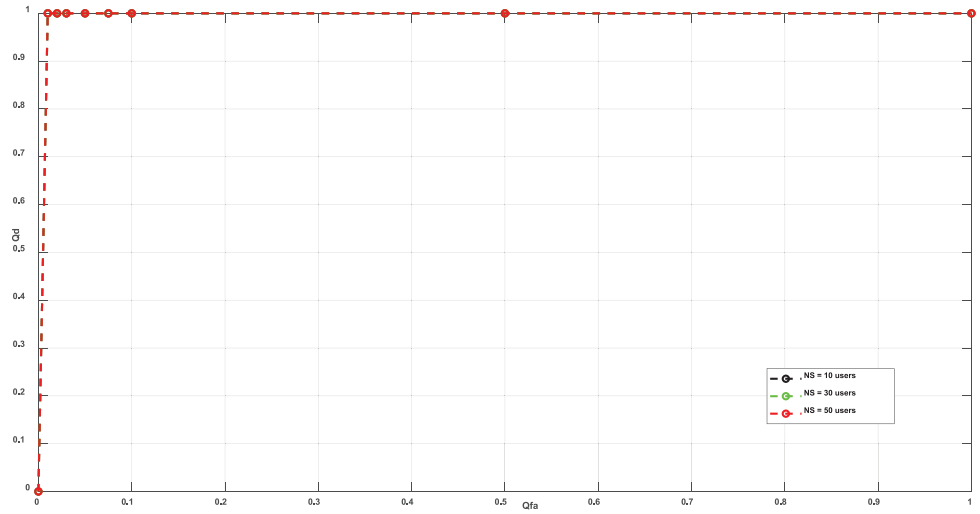

Fig. 13. The detection performance of proposed SS for UFMC-MIMO with centralized cooperative users.

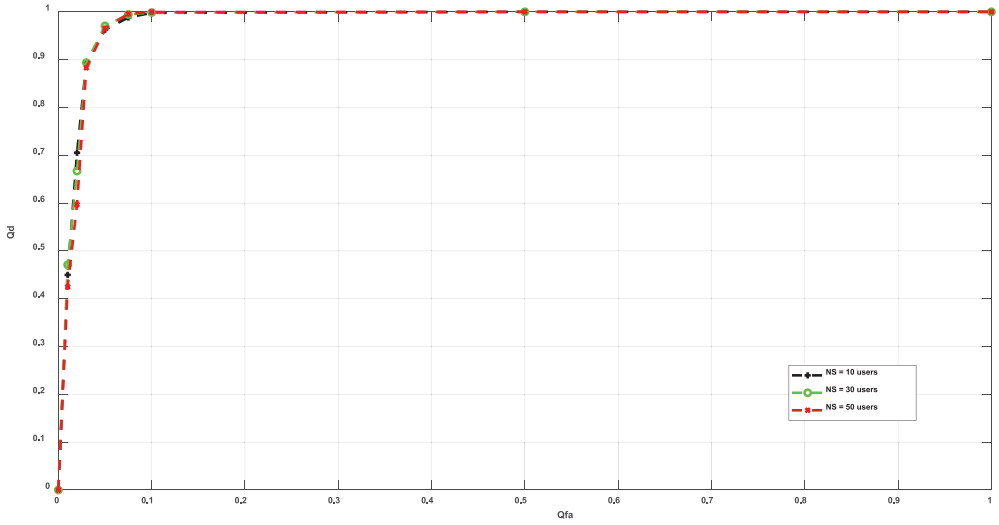

Fig. 14. The detection performance of proposed SS for FBMC-MIMO with centralized cooperative users.

Table 3
A Comparison of Parameters of Proposed System vs. Related Works.

Proposed and Related Works	ROC: (P_{fa}, P_d) for one users) ((Q_{fa}, Q_d) for many users)	P_e	SNR / dB
5G-NOMA [6]	0.04, 0.97	0.07	−5
Hybrid Gaussian Mixture Model [7]	0.064, 0.93	0.134	N/A
MFD [8]	0.05, 0.99	0.06	+15
Kernel-Gaussian noise [9]	0.09, 0.99	0.1	−8
ED-OFDM [10]	0.05, 0.61	0.44	−15
	0.01, 0.98 (with 5 × 5 antennas)	0.03	
5G-MIMO Detection (**1 user**) (only 2 × 2 antennas)	0.05, 0.95 (F-OFDM)	0.1	−20
	0.05, 0.96 (UFMC)	0.09	
	0.05, 0.98 (FBMC)	0.07	
5G-MIMO Detection (**50 users**) (only 2 × 2 antennas)	0.01, 0.99 (F-OFDM)	0.02	−20
	0.01, 0.995 (UFMC)	0.015	
	0.03, 0.9 (FBMC)	0.13	

SNR. The result is better for higher number of SUs comparing to lower number of SUs. On the other hand, Fig. 13 presents the detection performance for UFMC-MIMO system. All curves are conflict due to short signal length for different SUs rate. Fig. 14 described the detection performance of the FBMC-MIMO system. It is better for 50 SUs related to other kinds that has 10 and 30 SUs.

All in all, the obtained results of the proposed SS technique for MIMO centralized cooperative users are better than that of the proposed SS technique for MIMO non-cooperative users since the detection performance is improved once the number of SU increased.

4.3. The proposed system versus related works comparison

According to obtained results, the proposed SS technique for MIMO delivered better results than that of related works for both centralized cooperative and non-cooperative users. Table 3 summarizes numerical results of the proposed system and the related works. For system of non-cooperative users, the proposed system obtained results that are better than that of the related works. The proposed system for the FBMC waveform with 2×2 MIMO antennas has the best performance with fewer number of antennas. Its performance got on 98% detection percentage. In addition, for system of centralized cooperative users, the obtained results of proposed system are better than that of the related works. The proposed system for the F-OFDM and UFMC waveforms with 2×2 MIMO antennas have the best performance with fewer number of antennas. The detection probability is equal and greater than 0.99 for both kind of waveforms F-OFDM and UFMC, respectively.

In summary, the detection performance of proposed MIMO sensing system for centralized cooperative users is better than that of the proposed MIMO sensing system for only one user. It can be exploited for many 5G waveforms such as F-OFDM, FBMC, and UFMC.

5. Conclusion

In this paper, the performance of the SS technique for both non-cooperative and centralized cooperative (secondary users) methods. Both systems were performed for the 5G-MIMO communications system with a number of antennas for both transmitter and receiver. Three kinds of 5G systems has been analyzed; F-OFDM-MIMO, UFMC-MIMO, and FBMC-MIMO systems. The mathematical expressions are proposed for various numbers of secondary users, transmitter and receiver antennas, length of signal, and waveform shapes. Besides, developing the impact of test statistic and signal length rather than the expressions of detection for false alarm probabilities for both centralized cooperative and non-cooperative users are analyzed too. The obtained results of simulation for different number of samples, different values of SNRs, and the modulation types. The proposed system overcome the issues of low SNRs, and F-OFDM-MIMO, UFMC-MIMO, and FBMC-MIMO systems. The best results are obtained as follows; probability of detection for one only user are equal to 0.98 and 0.995 for FBMC (for one user) and UFMC (for 50 users), respectively. On the other hand, the increased number of antennas enhanced the detection performance in comparison with other detection systems that are did not use the MIMO technique.

Declaration of Competing Interest

The authors declare that they have no known competing financial interests or personal relationships that could have appeared to influence the work reported in this paper.

Acknowledgments

This work is supported by Universiti Putra Malaysia.

References

[1] Ansari J, Andersson C, de Bruin P, Farkas J, Grosjean L, Sachs J, et al. Performance of 5G trials for industrial automation. Electronics 2022;11(3):412.
[2] Pandit S, Singh G. Spectrum sensing in cognitive radio networks: potential challenges and future perspective. In: Pandit S, Singh G, editors. Spectrum Sharing in Cognitive Radio Networks. Cham: Springer International Publishing; 2017. p. 35–75.
[3] Bhattacharjee S, Acharya T, Bhattacharya U. Cognitive radio based spectrum sharing models for multicasting in 5G cellular networks: a survey. Comput Netw 2022;208:108870.
[4] Kumar A, Thakur P, Pandit S, Singh G. Analysis of optimal threshold selection for spectrum sensing in a cognitive radio network: an energy detection approach. Wirel Netw 2019;25(7):3917–31.
[5] Wang N, Wang Pu, Alipour-Fanid A, Jiao L, Zeng K. Physical-layer security of 5G wireless networks for IoT: challenges and opportunities. IEEE Internet Things J 2019;6(5):8169–81.
[6] Yasrab T, Gurugopinath S. Spectral efficiency of MIMO-NOMA cognitive radios with energy-based spectrum sensing. IEEE International Conference on Distributed Computing, VLSI, Electrical Circuits and Robotics (DISCOVER), 2019.
[7] Chowdary KU, Rao BP. Hybrid mixture model based on a hybrid optimization for spectrum sensing to improve the performance of MIMO–OFDM systems. Int J Pattern Recognit Artif Intell 2020;34(07):2058008.
[8] Singh J, Shukla A. Spectrum sensing in MIMO cognitive radio networks using likelihood ratio tests with unknown CSI. In: Intelligent Communication, Control and Devices. Springer; 2020. p. 185–93.
[9] Zhang J, Liu L, Liu M, Yi Y, Yang Q, Gong F. MIMO spectrum sensing for cognitive radio-based Internet of things. IEEE Internet Things J 2020;7(9):8874–85.
[10] Lorincz J, Ramljak I, Begusic D. Algorithm for evaluating energy detection spectrum sensing performance of cognitive radio MIMO-OFDM systems. Sensors 2021;21(20):6881.
[11] Lorincz J, Ramljak I, Begušić D. Performance analyses of energy detection based on square-law combining in MIMO-OFDM cognitive radio networks. Sensors 2021;21(22):7678.
[12] Lorincz J, Ramljak I, Begušić D. Analysis of the impact of detection threshold adjustments and noise uncertainty on energy detection performance in MIMO-OFDM cognitive radio systems. Sensors 2022;22(2):631.
[13] Taher MA, Radhi HS, Jameil AK. Enhanced F-OFDM candidate for 5G applications. J Ambient Intelligence Humanized Comput 2021;12(1):635–52.
[14] Sakkas L, Stergiou E, Tsoumanis G, Angelis CT. 5G UFMC scheme performance with different numerologies. Electronics 2021;10(16):1915.
[15] Liu Z, Xiao P, Hu S. Low-PAPR preamble design for FBMC systems. IEEE Trans Veh Technol 2019;68(8):7869–76.
[16] Kansal P, Gangadharappa M, Kumar A. An efficient composite two-tier threshold cooperative spectrum sensing technique for 5G systems. Arab J Sci Eng 2022;47(3):2865–79.
[17] Kumar A, Saha S. A decision confidence based multiuser MIMO cooperative spectrum sensing in CRNs. Phys Commun 2020;39:100995.
[18] Martínez DM, Andrade ÁG. Performance evaluation of welch's periodogram-based energy detection for spectrum sensing. IET Commun 2013;7(11):1117–25.
[19] Liu X, Sun Q, Lu W, Wu C, Ding H. Big-data-based intelligent spectrum sensing for heterogeneous spectrum communications in 5G. IEEE Wirel Commun 2020;27(5):67–73.
[20] Guimarães D. Gini index inspired robust detector for spectrum sensing over Ricean channels. Electron Lett 2018;55(12):713–4.
[21] Hu F, Chen B, Zhu K. Full spectrum sharing in cognitive radio networks toward 5G: A survey. IEEE Access 2018;6:15754–76.
[22] Wang H. Sparse channel estimation for MIMO-FBMC/OQAM wireless communications in smart city applications. IEEE Access 2018;6:60666–72.
[23] Wang G, Wang X, Zhao C. An iterative hybrid harmonics detection method based on discrete wavelet transform and Bartlett-Hann Window. Appl Sci 2020;10(11):3922.
[24] Grujić DN. Comments on ''generalized adaptive polynomial window function''. IEEE Access 2021;10:441–2.